pubs.acs.org/acschemicalbiology

Article

Breaking the Myth of Enzymatic Azoreduction

Yu-Ju Peng, Bing Xu, and Steven E. Rokita*

Cite This: *ACS Chem. Biol.* 2025, 20, 229−237

Read Online

ACCESS | Metrics & More | Article Recommendations | Supporting Information

ABSTRACT: Flavin-dependent azoreductases have been applied to a wide range of tasks from decolorizing numerous azo dyes to releasing azo-conjugated prodrugs. A general narrative reiterated in much of the literature suggests that this enzyme promotes sequential reduction of both the azo-containing substrate and its corresponding hydrazo product to release the aryl amine components while consuming two equivalents of NAD(P)H. Indeed, such aryl amines can be formed by incubation of certain azo compounds with azoreductases, but the nature of the substrates capable of this apparent azo bond lysis remained unknown. We have now prepared a set of azobenzene derivatives and characterized their turnover and products after treatment with azoreductase from *Escherichia coli* to discover the structural basis regulating aryl amine formation. Without resonance donation by aryl substituents, reduction ceases at the hydrazo product. This indicates that azoreductases do not act on the hydrazo bond. Instead, aryl amine formation depends on a spontaneous hydrazo bond lysis that is promoted by resonance stabilization and subsequent reduction of the quinone-like intermediate by azoreductase. Experimental and computational approaches confirm the substituent dependence of this process. With knowledge of this requirement, full release of aryl amines from azo-conjugates can now be designed and applied with confidence.

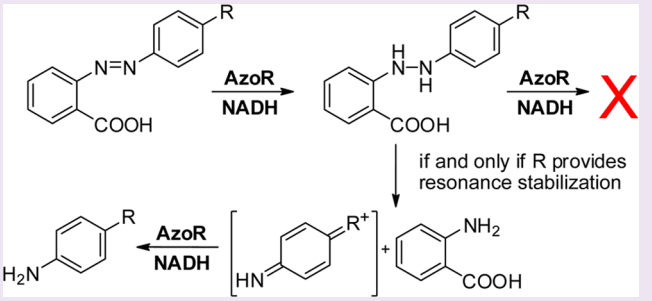

INTRODUCTION

Azobenzene was first reported almost 200 years ago and discovery of the first azo dye, aniline yellow, soon followed.[1] More recently, azobenzene derivatives have been used to create optical materials, photoswitches, molecular machines, and self-immolative polymers.[1] The first synthetic antibiotic prontosil featured an azo group as well. Upon reduction of this group in vivo, an active sulfanilamide antibiotic is released (Figure 1). Since this discovery, the azo group has been integrated into a broad range of prodrugs including balsalazide and related derivatives for treating ulcerative colitis.[2] An equivalent prodrug strategy has also been successfully extended to anticancer drugs such as gemcitabine (Figure 1C), methotrexate, and a platinum complex.[3] In each case, drug release depends on the ability of an azoreductase to transform the azo substrate to its corresponding aniline products.[4] This activity is commonly conferred by our microbiota and consequently incorporation of an azo appendage serves as a very convenient approach for releasing therapeutic compounds into our colon. As a corollary, azo dyes are subject to a similar reduction, but their metabolites can be toxic and carcinogenic.[5,6] The potential for generating deleterious products has not deterred the application of azoreductases in the environment for bioremediation of industrial waste streams.[7−9] Further applications of azoreductase involve the incorporation of azo groups into the design of cleavable linkers in proteomics,[10] biosensors in living cells[11] and traceable drug delivery.[12]

Azoreductases are broadly distributed in nature although most studies have focused on those from aerobic prokaryotes.[4,6,13] These variously use NADH or NADPH to reduce a bound flavin mononucleotide (FMN) within a flavodoxin-like fold. The reduced flavin in turn transfers a hydride equivalent to form a presumptive hydrazo intermediate that is rarely detected (Figure 1B).[14] This in turn may generate two amine products with the consumption of a second equivalent of NAD(P)H. Crystal structures of a variety of azoreductases are available and describe a rather large and accessible active site that can accommodate a wide variety of azo dyes in agreement with kinetic studies.[5,13] Although amine products were identified from the reduction of various azo substrates by azoreductases, no formal examination of the catalytic mechanism has been published to our knowledge. Typically, enzyme participation is invoked or presumed during the reduction of both the azo-containing substrate and its hydrazo intermediate.[14,15] Two alternative pathways were proposed for the reduction of the azo prodrug balsalazide including one that involved a nonenzymatic decomposition of the hydrazo intermediate. This was suggested after crystallographic analysis

Received: November 15, 2024
Revised: December 10, 2024
Accepted: December 12, 2024
Published: December 21, 2024

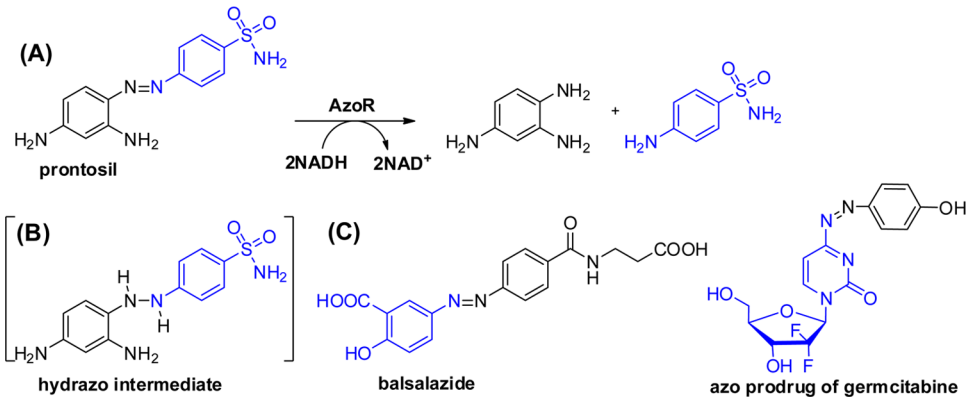

Figure 1. Enzymatic azoreduction and azoreductase-activated prodrugs. (A) Reduction of prontosil by AzoR, (B) an implied hydrazo intermediate in reduction of prontosil, and (C) two representative azo prodrugs. The active therapeutics are highlighted in blue and released after reduction by azoreductase.

Scheme 1. Enzymatic Reduction of 4-FCH$_2$-Azo by AzoR[a]

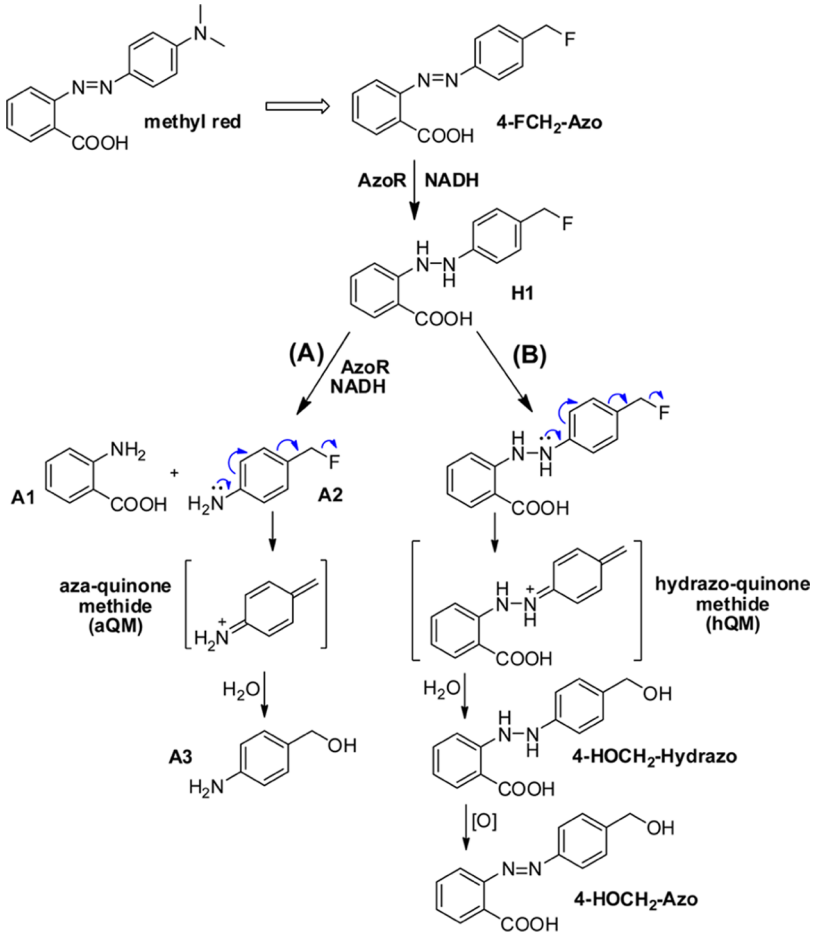

[a](A) Complete reduction to form **aQM** and (B) reduction halted at the hydrazo intermediate and subsequent elimination, addition, and oxidation to form **4-HOCH$_2$-Azo**.

revealed a surprising misalignment between balsalazide (Figure 1C) and the flavin of an azoreductase.[4,16] Without context, this observation remains ambiguous since active site binding geometry is not necessarily indicative of mechanism or regiochemistry as evident from the nonproductive alignment of various substrates in the active site of FMN-dependent nitroreductases.[17,18] Still, lysis of the hydrazo bond was also thought to occur spontaneously for certain examples after incubating azo dyes with cytochrome P450.[19]

Our interest in azoreductase derived from a desire to generate azaquinone methide intermediates (**aQM**) enzymatically for alkylation of biological macromolecules. Only limited information on the reactivity of these electrophiles under physiological conditions was available in comparison to the extensive literature on the analogous quinone methides.[20−23]

https://doi.org/10.1021/acschembio.4c00779
ACS Chem. Biol. 2025, 20, 229−237

Without definitive instruction from the literature on azoreductases, we assumed a fluoromethyl derivative (**4-FCH$_2$-Azo**) of the common azoreductase substrate methyl red would generate a transient *para*-fluoromethyl aniline (**A2**) that rapidly eliminates to form the *para* **aQM** (Scheme 1). Instead, no reduction was observed beyond the hydrazo intermediate as described below. Motivated by this unsuccessful design, we aimed to create guidelines for reliable release of the amine components from azo compounds by examining the substituent dependence of product formation. This report demonstrates through experimental and computational methods that resonance donation by *ortho* or *para* substituents is a prerequisite for nonenzymatic lysis of the hydrazo bond. The azoreductase from *Escherichia coli* consumes one equivalent of NADH to generate the hydrazo intermediate and one equivalent of NADH to reduce the quinone-like intermediate formed after spontaneous decomposition of the hydrazo intermediate. The hydrazo bond is not subject to direct reduction by the azoreductase.

RESULTS AND DISCUSSION

Unexpected Products Formed by Azoreduction of a Fluoromethyl-Substituted Azobenzene. Methyl red is used as a reliable substrate for characterizing azoreductases from numerous organisms based on its model behavior and ease of assay.[7,13,24] 2-Aminobenzoic acid and 4-(dimethylamino)aniline have been confirmed as the products of its reduction by azoreductase as expected for the full conversion of an azo group to its component aryl amines.[25,26] These products attracted our attention for generating **aQM** intermediates through an enzyme-controlled reduction. Release of a suitably prepared aniline derivative would produce an **aQM** in a complementary process to hydrolysis of acylated aniline derivatives.[27,28] A fluoromethyl group was selected here to minimize the potential of direct nucleophilic substitution at the benzylic position prior to enzymatic generation of the anticipated **aQM** precursor (Scheme 1). The desired **4-FCH$_2$-Azo** was constructed using a Baeyer−Mills reaction that couples an aryl amine to a nitrosoarene (see below and the Supporting Information).[29,30] Azoreductase from *E. coli* (AzoR) was selected as a prototypical azoreductase based on its availability through *in situ* PCR and prior characterization that included crystal structures of its oxidized, reduced, and ligand-bound forms.[24,31]

Routine incubation of **4-FCH$_2$-Azo** with AzoR and NADH under neutral conditions generated two products detected by LC-MS (Scheme 1 and Figure S1). No lysis of the azo bond was detected. Instead, **4-HOCH$_2$−Hydrazo** was observed and thought to form by water addition to a hydrazo-quinone methide (**hQM**) produced upon spontaneous elimination of HF from the hydrazo product (**H1**) (Scheme 1). **4-HOCH$_2$-Azo** was also observed and likely derived from spontaneous oxidation of **4-HOCH$_2$−Hydrazo** by ambient O_2.[32] This latter product was not the result of direct substitution at the benzylic position since **4-FCH$_2$-Azo** was inert to equivalent incubations lacking AzoR and NADH (Figure S1).

The carboxylic substituent is common to methyl red and **4-FCH$_2$-Azo** and thus not implicated in the resistance of **4-FCH$_2$-Azo** to full reduction and release of the anticipated aniline derivative (**A2**, Scheme 1). Thus, the replacement of the electron-rich dimethylamine with the fluoromethyl group most likely caused the unexpected product profile. This result suggested that the criteria for prodrug release by azoreduction was not sufficiently characterized by prior literature and likely required inductive or resonance contributions from an electron-donating group (EDG). To test this hypothesis, a series of azobenzene derivatives has now been synthesized with a range of substituents and characterized with AzoR.

Design and Synthesis of Azobenzenes to Correlate Substituent Effects and Product Profiles Generated from Azoreduction Promoted by AzoR. To provide a systematic correlation between aryl substituents and azo bond lysis, substrates were designed to vary the inductive and resonance contributions. Initially, the dimethylamino group of methyl red was replaced by hydroxyl (HO), methoxy (MeO), N-acetylamino (AcHN), methyl (Me), and cyano (NC) groups and the carboxylate group was retained for water solubility and enzyme recognition. Baeyer−Mills reactions were again performed to construct the key azo bonds (Scheme 2).[29,30] In this reaction, the aniline derivatives serve as nucleophiles to react with the electrophilic nitrosoarene. Typically, EDGs on the aniline component promote coupling and likewise, electron-withdrawing groups (EWGs) suppress reaction.[33] Therefore, the nitrosoarene was generated from the aryl nitrile to maximize the yield of **4-NC-Azo** (Scheme 2A). Conversely, a nitrosoarene of the methyl benzoic acid component was coupled to the aniline derivatives with EDGs (Scheme 2B). In both strategies, the nitrosoarenes were synthesized by oxidization of the corresponding amines with Oxone^{tm}. As a final step, the methyl esters were hydrolyzed under basic conditions to provide the desired substrates for AzoR (Supporting Information).

Scheme 2. Synthetic Strategies to Access Azobenzenes with (A) an Electron-Withdrawing Group (NC) and (B) Electron-Donating Groups (R = HO, MeO, AcHN, Me)[a]

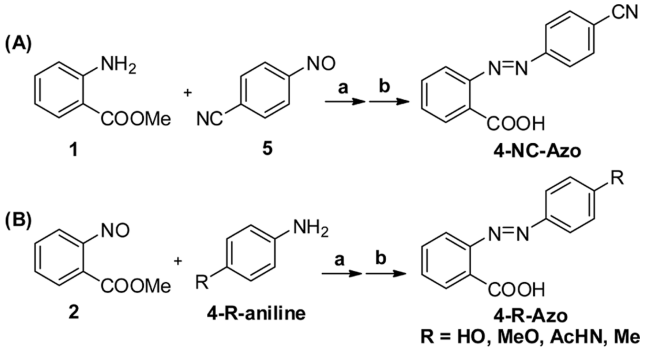

[a]a. AcOH, rt; b. NaOH, MeOH, 60 °C. For details, see the Methods section and the Supporting Information.

Catalytic Efficiency and Binding Affinity of AzoR for 4-R-Azo. The set of potential substrates described above were first assessed for their turnover and binding with AzoR to provide the necessary context for subsequent product studies. **4-R-Azo** consumption was monitored over time using reverse-phase (C18) HPLC analysis and shown to proceed linearly over the time required for determining catalytic efficiency (Figure S2). The substrate dependence of catalysis was next measured by varying **4-R-Azo** concentration with a fixed concentration of NADH (200 μM) in 25 mM Tris pH 7.4 with 50 mM NaCl and 5% DMSO (Figure S3). The catalytic efficiencies (k_{cat}/K_m) for **4-R-Azo** consumption are quite similar (20−36 × 10^3 M^{-1} s^{-1}) except for **4-Me-Azo** that was consumed at a 3- to 5-fold lower efficiency (7 × 10^3 M^{-1} s^{-1})

https://doi.org/10.1021/acschembio.4c00779
ACS Chem. Biol. 2025, 20, 229−237

(Table 1 and Figure S3). In general, substituents at the C4 position had minimal impact on the initial rate of catalysis. A greater influence of these substituents is evident in the affinity of **4-R-Azo** for AzoR. These measurements relied on the ability of substrates to quench the fluorescence of the oxidized form of FMN. Subsequent catalysis is prevented since the oxidized FMN requires reduction prior to turnover. The K_d of **4-R-Azo** spanned over almost a 7-fold range but did not correlate with catalytic efficiency nor substituent size or polarity (Table 1 and Figure S4). Greatest affinity was measured for **4-AcHN-Azo** while the weakest affinity was measured for **4-NC-Azo**. Molecular docking of this set of substrates based on a crystal structure of AzoR (PDB: 2z98) was performed using AutoDock Vina[34] to rationalize the relative affinities for the active site. Binding of 4-AcHN group included polar interactions with the backbone amide of Ala-114 (2.9 Å) and the hydroxyl group of Tyr-120 (3.0 Å) that are not shared with the other substituents (Figure S5). In contrast, key interactions between the azo nitrogens and Tyr-120 (3.3 and 4.0 Å) are common to all of the substrates although previous mutagenesis studies suggested that Tyr-120 was more influential for binding NADH than methyl red.[24]

Table 1. Binding Affinity and Catalytic Efficiency of AzoR with Substituted Azobenzene Derivatives[a]

4-R-Azo	binding and kinetic parameters		products[c]		substituent constant[d]	
R	K_d (μM)	k_{cat}/K_m (M^{-1} s^{-1}) × 10^3	hydrazo	anilines	σ_I	σ_R
Me_2N	N/A[b]	100 ± 4	−	+	0.15	−0.98
HO	240 ± 10	20 ± 1	−	+	0.33	−0.70
MeO	370 ± 40	36 ± 2	+	+	0.29	−0.56
AcHN	67 ± 5	21 ± 1	+	+	0.31	−0.31
Me	400 ± 60	7 ± 1	+	−	0.01	−0.18
NC	450 ± 40	20 ± 1	+	−	0.51	0.15

[a]Data represents an average of three independent measurements and their uncertainty is the standard deviation. For details, see the Methods section and the Supporting Information. [b]Could not be measured due to interference by the absorbance of the substrate. [c]Reactions were performed for 3 h at 25 °C with 100 μM substrate, 200 μM NADH, and 20 nM AzoR in 25 mM Tris pH 7.4, 50 mM NaCl, and 5% DMSO (25 °C). Products were detected by LC-MS; +, detected; −, not detected. [d]Inductive parameter (σ_I) and resonance effects parameter (σ_R) from ref 35.

Product Identification of Azoreduction. Products of AzoR catalysis were identified by LC-MS to learn the structural criteria for limiting transformation to a hydrazo derivative or allowing full lysis of the azo bond to release the corresponding aryl amines. Substituent effects had not previously been examined to identify the role of electronics in this dichotomy but our initial observations already indicated that the 4-FCH_2 group was insufficient to generate the amine products (Scheme 1). The **4-R-Azo** series was designed to test a range of resonance and inductive contributions. Those with electron pairs readily available for resonance donation (R = Me_2N and HO) generated the aryl amines exclusively as commonly expected from the literature (Table 1 and Figure S6).[25,26] Substituents with a lesser tendency for resonance donation (R = MeO and AcHN) yielded a mixture of the hydrazo and amino products under equivalent conditions and finally the electron-donating and -withdrawing substituents lacking resonance contributions (R = Me and NC) were limited to the hydrazo products without detectable formation of their component amines (Figure S7). As illustrated by this trend, resonance contributions are a key determinant of the product profile. This is further supported by the general correlation between the reaction products and the substituent resonance constants (σ_R) of the functional group at the 4-position (Table 1).[35] No equivalent pattern was evident for the inductive constants (σ_I, Table 1). Likewise, redox potential does not appear to influence turnover of this series of substrates. The most readily reduced substrate should be that containing the strongest EWG,[36] **4-NC-Azo**, but this was not reduced to its hydrazo product with the greatest catalytic efficiency nor did it form its amino products (Table 1). Future design of azo-conjugated prodrugs should include an EDG constituent capable of strong resonance donation to ensure release of the desired amino product.

Chemical reduction of **4-HO-Azo** and **4-Me-Azo** by sodium dithionite (10 equiv) yielded equivalent results to those generated by AzoR. The azo bond lyzed to yield its amine product **A1** for the resonance-stabilized **4-HO-Azo** but only the hydrazo product was formed by **4-Me-Azo** (Figure S8). Collectively, these results are best explained by one of the previously untested conjectures that the hydrazo product spontaneously decomposes in an enzyme-independent process.[16,19] Conversion of **4-R-Azo** to its hydrazo derivative by AzoR is invariant to the R group but subsequent hydrazo bond lysis requires the R group to provide stabilization for a developing positive charge to allow formation of the electron-deficient benzoquinone imine (Scheme 3A). This scheme is consistent with the dominant effect of resonance contributions and lack of correlation to the reduction potentials of the substrates. The second equivalent of NADH consumed in the standard methyl red reaction is not involved in reduction of the hydrazo bond but rather in an AzoR-dependent reduction of the quinone intermediate (see below).

Scheme 3. . Proposed Mechanism of Azo Bond Lysis and Formation of Its Two Aryl Amine Products[a]

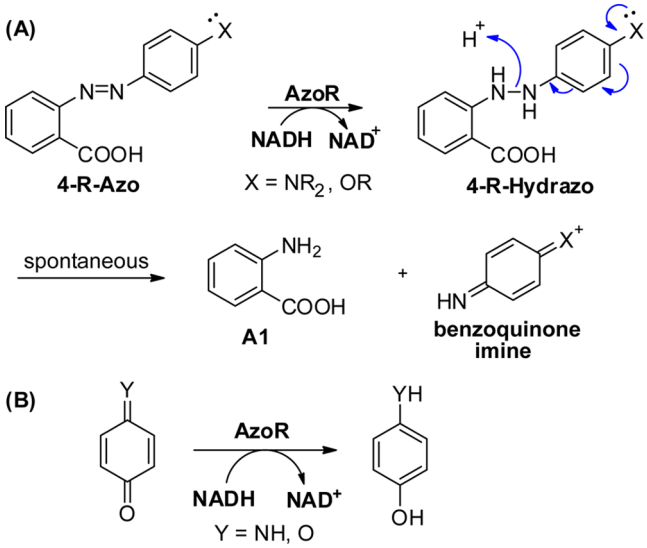

[a](A) Enzymatic reduction to form a hydrazo product. (B) Subsequent enzymatic reduction of a transient quinone to consume the second equivalent of NADH.

https://doi.org/10.1021/acschembio.4c00779
ACS Chem. Biol. 2025, 20, 229−237

Confirmation That Resonance Donation Is the Principal Determinant for Complete Lysis of the Azo Bond after Initial Formation of the Hydrazo Product by AzoR. As a complementary approach to demonstrate the significance of resonance donation in product determination, the hydroxyl group of **4-HO-Azo** was shifted to the *meta* (**3-HO-Azo**) and *ortho* (**2-HO-Azo**) positions. All of these provide the inductive effects of a hydroxyl group but only substitution at the 2- and 4-positions allows for the resonance stabilization that is suggested above to be critical for amine formation (Scheme 3). The two new derivatives were synthesized in analogy to those of the **4-R-Azo** series (Scheme S3).[29,30] Their affinity for the oxidized form of AzoR was in the range of those measured for the **4-R-Azo** series with K_d values of 210 and 140 μM for the **3-HO-Azo** and **2-HO-Azo** isomers, respectively (Figure S4). However, neither was consumed by AzoR as efficiently as the **4-R-Azo** series. The k_{cat}/K_m for **3-HO-Azo** was 40% lower than that of **4-Me-Azo**, the slowest of the series and the k_{cat}/K_m for **2-HO-Azo** was 2.6-fold lower than that of **4-Me-Azo** (Figure S3). Still, both were processed by AzoR to yield the anticipated products that are dictated by resonance contributions. Incubation of **3-HO-Azo** under standard conditions with 200 μM NADH and AzoR yielded only its hydrazo product as observed by LC-MS (Figure S9). In contrast, no hydrazo product was detected after an equivalent incubation of **2-HO-Azo** with AzoR and instead its amine **A1** and 2-hydroxyaniline were evident (Figure S9). Since the 2-aminobenzoic component is invariable in this investigation, the product profile must be controlled by the differing hydroxy group positions. Again as proposed above, release of aryl amine from a complete lysis of the azo bond requires substituents to labilize the hydrazo bond and strongly stabilize the electron-deficient intermediate through resonance (Scheme 3).

Benzoquinones as Substrates for AzoR to Form a Reduced Product. No evidence suggests that the hydrazo products of AzoR reaction are reduced by AzoR. For example, the hydrazo derivatives generated from **4-Me-Azo, 4-NC-Azo**, and **3-HO-Azo** persist in the presence of AzoR and NADH. Still, two equivalents of NADH are consumed when lysis of the azo bond leads to the release of its two amine components.[13,16] The first NADH drives the FMN-dependent conversion of the azo substrate to its hydrazo product and the second NADH is expected to drive a subsequent FMN-dependent reduction of a benzoquinone imine intermediate to its hydroquinone product (Scheme 3B). Azoreductases, like nitroreductases, are known to promote a variety of reactions in addition to their namesakes including quinone reduction,[13,37−40] and thus, azoreductase also likely catalyzes the cryptic reduction of the intermediate cation to its stable aniline product.

Attempts were made to synthesize benzoquinone imine to test if AzoR could catalyze its reduction. Unfortunately, oxidation of 4-aminophenol with silver(I) oxide[41] did not provide an isolable product after multiple trials. This is consistent with the rapid decomposition of its N-acetylated derivative with a half-life of ∼11 min in 0.1 M sodium phosphate pH 4.0.[42,43] As an alternative, *para*-benzoquinone was selected as a model substrate to measure the relative propensity for AzoR to promote quinone versus azo bond reduction. AzoR (330 nM) fully converted *para*-benzoquinone (500 μM) to its hydroquinone product within 2 min in the presence of NADH (500 μM) (Figure S10). This reaction was enzyme-dependent and had a catalytic efficiency (k_{cat}/K_m) greater than 3.7×10^6 M^{-1} s^{-1}, a magnitude 3 orders more than that of the initial azoreduction (Table 1 and Figure S11). If the rate of quinone reaction is driven in part by reduction potential, then turnover of *para*-benzoquinone imine would likely have proceeded even faster than that observed for *para*-benzoquinone since the reduction potential of the former ($2e^-/2H^+$, E = 0.79 V vs NHE) is higher than the later ($2e^-/2H^+$, E = 0.64 V vs NHE).[44,45] Accordingly, azoreduction and not quinone reduction is likely rate-determining for the overall turnover of AzoR. Accumulation of a quinone intermediate appears negligible after spontaneous and fast hydrazo bond lysis (Scheme 3).[14]

Assessing Spontaneous Hydrazo Bond Lysis with DFT Calculations. The oxidative lability of hydrazobenzenes in the presence of O_2[32] and the decomposition of some of its 2- and 4-substituted derivatives described above complicate direct experimental approaches to identify the structural and electronic requirements for spontaneous N−N bond lysis. As an alternate, computational methods were applied to examine hydrazo bond lysis and predict which hydrazo compounds are inclined to lyse spontaneously.

Hydrazobenzene (**HAB**) and 4-hydroxyhydrazobenzene (**4-HO-HAB**) were used as model compounds to investigate the requirements for facile N−N bond lysis (Scheme 4).

Scheme 4. Spontaneous Lysis of a (A) Neutral and (B) Protonated Form of Hydrazobenzene (R = H, HAB) and 4-Hydroxyhydrazobenzene (R = HO, 4-HO-HAB)

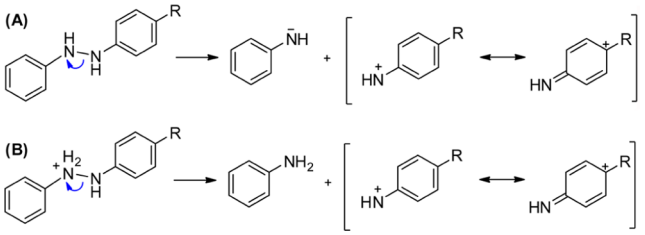

Differences between the Gibbs free energies of the hydrazo intermediate and its lysis products were used to estimate the propensity for reaction of the neutral and protonated species. Lysing the neutral **HAB** and **4-HO-HAB** (Scheme 4A) is highly endothermic with ΔG values of 81 and 62 kcal/mol (Table S1), respectively. Such transformations would be very unlikely under standard laboratory conditions. The lack of reaction for the neutral species was further confirmed by the absence of a defined transition state (TS) for dissociation of the N−N bond as the potential energy surface was scanned with increasing N−N bond lengths. This analysis was stopped at a N−N distance of 3.39 Å (Figure 2A) beyond which no TS is likely to exist. Within this scope, a TS would have been indicated by a decrease in the energy of the nascent intermediates. The enthalpic barriers (ΔE) of N−N bond lysis remain very similar to the free energy of reaction, ΔG. Therefore, neither the neutral **HAB** nor the neutral **4-HO-HAB** decomposes spontaneously. In both cases, the high energy of transformation can be ascribed to the necessary charge separation and aniline anion formation.

An alternative mechanism could involve protonation of the hydrazo bond to avoid formation of the nascent aniline anion. While the pK_a of azobenzene is low (estimated between −2.5 and −1.6),[46,47] its basicity would increase dramatically as the departing nitrogen becomes electron-rich. The energy

https://doi.org/10.1021/acschembio.4c00779
ACS Chem. Biol. 2025, 20, 229−237

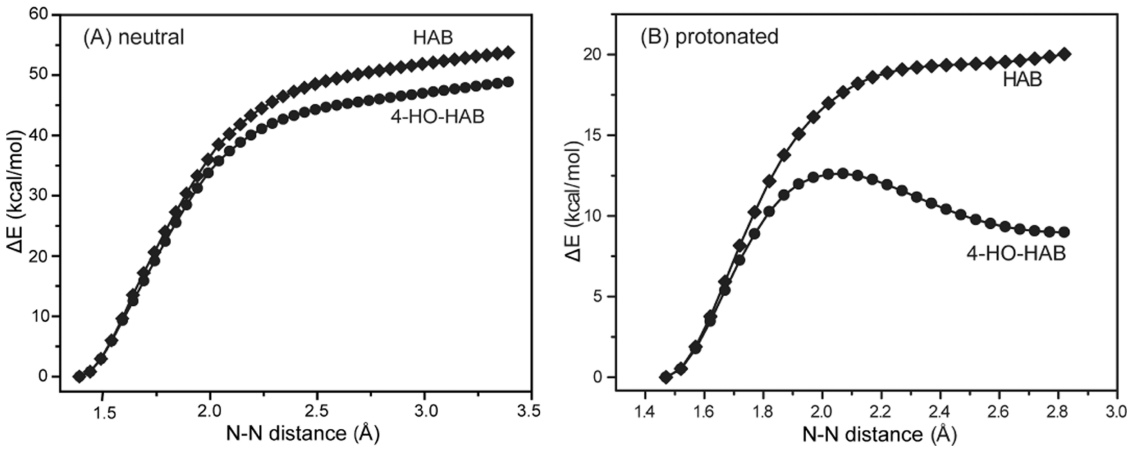

Figure 2. Lysis of the N−N bond in (A) neutral and (B) protonated **HAB** and **4-HO-HAB** was simulated by relaxed scans for which the relative energy (ΔE) was measured as the N−N bond length was increased stepwise from the optimized structure (0.05 Å increase per step, 40 steps) using the DFT method (M06-2X//6-311G++**//IEFPCM,water).

associated with lengthening of the N−N bond was then also calculated for the protonated **HAB** and protonated **4-HO-HAB** in search of a reasonable TS (Scheme 4B). Again, a continual increase in energy (ΔE) was generated as the N−N distance increased for the protonated **HAB** suggesting no TS (Figure 2B). In contrast, elongating the N−N bond of the protonated **4-HO-HAB** exhibited an increase and then decrease of ΔE as expected when passing through a TS. In this case, an N−N distance of 2.07 Å presented a maximum ΔE of less than 13 kcal/mol for **4-HO-HAB**, a value significantly lower than the maximum ΔE of **HAB** (>20 kcal/mol). The preferential lysis of the protonated **4-HO-HAB** is consistent with full conversion of **4-HO-Azo** to its amine components while derivatives such as **4-Me-Azo** remain at the hydrazo level after incubation with AzoR and NADH (Table 1).

The thermodynamic and kinetic barriers for the range of substituents in the **4-R-Azo** series were next calculated for their protonated form and compared to the experimental results above (Table 2). N−N bond lysis remained unfavorable for hydrazo compounds lacking resonance stabilization (R = Me, NC). Neither substituent stabilizes the electron-deficient intermediate to allow for bond dissociation. With the contributions of the Me_2N, HO, MeO, and AcHN groups at the 4-position, the ΔG decreases to 11 kcal/mol or less for the cationic intermediate. The value for the Me_2N substituent is most favorable. Reaction may also be favorable when the HO analog releases a dissociable proton. Neither the MeO or AcHN substituents can dissipate their positive charge by proton release and thus formation of the benzoquinone imine is limited based on their ΔG (Table 1).

Table 2. Thermodynamic Equilibria and Kinetic Barriers for Bond Lysis of Protonated Hydrazo Compounds[a]

substituent (R)	ΔG (kcal/mol)	$\Delta G^{\ddagger}$ (kcal/mol)
4-Me_2N	−8.8	6.0
4-HO	11	11
4-MeO	9.3	11
4-AcHN	9.7	13
4-Me	21	/
4-H	28	/
4-NC	37	/
3-HO	29	/

[a]Structures of starting hydrazo compounds, corresponding TS, and products were individually optimized using DFT (M06-2X//6-311G++**//IEFPCM,water). "/" suggests no TS.

Transition states are evident by computation for all azo derivatives containing resonance-donating substituents and their kinetic barriers are only slightly higher in general than the energy associated with the reaction intermediates. Based on the Eyring equation[48,49] and rate equation[50] for a first-order reaction, an activation free energy ($\Delta G^{\ddagger}$) of 11 kcal/mol (R = HO, MeO) suggests a half-life for the hydrazo product of 13 μs at 298 K. Thus, spontaneous and rapid N−N bond lysis is highly likely for R = Me_2N, HO, MeO, and AcHN. In agreement with the experimental data above, the energy gain (ΔG) and the kinetic barrier ($\Delta G^{\ddagger}$) increase significantly for a derivative containing a HO substituent at the 3-position compared to that at the 4-position. Thus, the experimental observations of the R-Azo series with azoreductase align with computational analyses of hydrazo intermediates and should guide future predictions on the product profiles for azoreductase catalysis.

CONCLUSIONS

Experimental and computational results described in this article break the myth surrounding enzymatic azoreduction. At least for AzoR, hydrazo bond lysis is not enzyme-dependent and not all azo substrates yield their two amine components after turnover. AzoR is responsible for the reduction of azo compounds to their hydrazo products and subsequent reaction relies on the resonance donation of substituents in conjugation with the hydrazo bond to promote its spontaneous lysis. Previously, participation of an EDG was suggested during studies with azobenzene derivatives and cytochrome P450 but no later investigations defined causality for hydrazo bond decomposition.[19] Similarly, a nonenzymatic lysis of the hydrazo bond was invoked to explain an unusual orientation of the azo-containing drug balsalazide (Figure 1) in a crystal structure with an azoreductase from *Pseudomonas aeruginosa*.[16] Again, no subsequent attention confirmed the catalytic activity of this orientation. Consequently, the literature predominantly repeated the expectation that azoreductases catalyze the reduction of both the azo and hydrazo bonds.[13]

https://doi.org/10.1021/acschembio.4c00779
ACS Chem. Biol. 2025, 20, 229−237

Here, we describe a systematic study to demonstrate the importance of resonance donation from aromatic substituents as the primary determinant of hydrazo bond lysis. The strength of a resonance contribution may now be used to predict the tendency for azoreductase to yield either a hydrazo product or release the two amine components of the original azo substrate. Furthermore, benzoquinone imines, rather than hydrazobenzene derivatives, are most likely the substrates that consume the second equivalent of NADH during AzoR catalysis. DFT calculations are consistent with the experimentally determined tendency for decomposition of hydrazo derivatives and together provide an opportunity *a priori* to design substrates that generate the desired product(s). For this, an activation free energy of less than 13 kcal/mol should predict at least fractional decomposition of the hydrazo product enabling release of the amine components. All commercial azo prodrugs, such as prontosil and olsalazine, and the azo prodrug of germcitabine (Figure 1C) contain functional groups for resonance donation at the appropriate positions for release of their medicinally active component. Whether these were generated by trial and error or through unpublished knowledge on the structure−activity relationship is not clear but now guidelines are available for future design of azo compounds for in vivo activation.

METHODS

General Strategy for Constructing Azo Bonds. An aqueous solution of Oxone^{tm} (8 eq., 0.8 M) was added quickly to a DCM solution of the chosen aryl amine (0.3 M). The mixture was stirred at RT under N_2 for 2 h. The crude mixture was then extracted with 20 mL DCM and washed sequentially with 20 mL of the following: 1 N HCl, satd. $NaHCO_3$, and brine. The organic phase was dried over anhydrous $MgSO_4$ and concentrated under reduced pressure. The crude product was directly used in the next step by adding AcOH to make a 0.15 M solution and combining this with the corresponding aniline (1.1 equiv) for azo bond formation. The reaction mixture was stirred at RT under N_2 for 16 h. The solvent was removed by rotary evaporation. The resulting residue was diluted with 20 mL EtOAc and washed with 20 mL 1 N HCl and 20 mL satd. $NaHCO_3$. The organic phase was dried over anhydrous $MgSO_4$ and concentrated under reduced pressure. The collected product was purified by silica column chromatography using solvent systems of hexane/EtOAc or DCM/EtOAc to give the desired azobenzene derivative. Full details are provided in the Supporting Information.

Expression and Purification of AzoR. *E. coli* Rosetta 2 (DE3) cells containing pET24a-AzoR-His6 (see the Supporting Information) were inoculated into LB medium (20 mL) with kanamycin (50 μg/mL) and incubated overnight at 37 °C with shaking (220 rpm). The culture was then diluted (1:50, v/v) into LB medium (0.5 L) with kanamycin (50 μg/mL) and incubated at 37 °C with shaking (220 rpm) for 3 to 5 h until the OD_{600} reached 0.60. After the culture was cooled below 18 °C in the refrigerator, isopropyl β-D-1-thiogalactopyranoside (IPTG) was added to a final concentration of 0.2 mM. Expression of the protein continued at 18 °C with shaking (220 rpm) for 20 h. Cells were harvested by centrifugation (5000*g*, 4 °C) for 30 min and stored at −80 °C.

Frozen cell pellets were thawed at RT and resuspended in ∼25 mL of lysis buffer (50 mM sodium phosphate pH 7.4, 500 mM NaCl, 10% glycerol, 25 mM imidazole) with a vortex mixer. FMN (∼300 mM) was added to the suspension to enhance its occupancy in AzoR. Cells were then lysed by an EmulsiFlex-C3 homogenizer (Avestin) with 3−4 passes at ∼17,000 psi. Cell debris was removed by centrifugation at 35,000*g* for 30 min and the supernatant was passed through nickel-nitrilotriacetic acid (Ni-NTA) resin (Thermo Fisher Scientific, pre-equilibrated with 3 column volumes of lysis buffer) by a benchtop Econo pump (Bio-Rad) at a flow rate of 1 mL/min. The Ni-NTA column was then attached to an ÄKTA protein purification system (GE Healthcare) and washed sequentially with 25, 60, and 80 mM imidazole in buffer B (50 mM sodium phosphate pH 7.4, 500 mM NaCl, 10% glycerol) for 2−3 column volumes each at a flow rate of 1 mL/min. The target protein was finally eluted with 250 mM imidazole in buffer B for 2−3 column volumes. The eluted protein was supplemented with ∼300 μM FMN and incubated on ice overnight to further increase the FMN occupancy. Finally, the solution was exchanged into storage buffer (50 mM Tris pH 7.4, 300 mM NaCl, 10% glycerol) using a gravity-driven PD-10 desalting column (GE Healthcare) following the manufacturer's instructions. This solution was concentrated with a 30 kDa molecular-weight cutoff centrifugal filter unit (Amicon), flash-frozen with liquid nitrogen in aliquots, and stored at −80 °C. The purified enzyme was analyzed by 12% SDS-PAGE with Coomassie brilliant blue staining. Enzyme concentration was determined by ultaviolet−visible (UV−vis) absorbance at 280 nm ($\varepsilon_{280\ nm}$ = 15,930 $M^{-1}cm^{-1}$, estimated by the ExPASy ProtParam tool) after correcting for the contribution from bound FMN (A_{280}/A_{450} = 1.57).[51] The FMN occupancy of the purified enzyme was estimated by the ratio of enzyme-bound FMN (determined by UV−vis at 450 nm, $\varepsilon_{450\ nm}$ = 12500 $M^{-1}cm^{-1}$ for FMN) over the total protein concentration.[51] A typical yield of azoreductase from a 250 mL cell culture was 32 mg with 65% FMN occupancy.

Product Identification after Enzymatic Reduction. Enzyme reactions were incubated in brown Eppendorf tubes with 100 μM substrate, 200 μM NADH, and 20 nM AzoR in buffer A (25 mM Tris pH 7.4, 50 mM NaCl, 5% DMSO) at 25 °C for 3 h without stirring. The enzyme was removed from the solution with an Amicon centrifugal filter (10 kDa MWCO), and the resulting filtrate was analyzed with a Waters Xevo UPLC-MS with electrospray ionization (ESI) and q-TOF MS/MS analyzer using a flow rate of 0.3 mL/min (see the Supporting Information for details).

Kinetic Assay for Azoreduction. The indicated concentration of azo substrates, 20 nM AzoR, and 200 μM NADH were incubated in buffer A at 25 °C. Tryptophan (100 μM) was added as internal standard for quantification, and then the reaction was quenched after 2−30 min by adding acetonitrile to a final concentration of 11%. Consumption of substrates was monitored by reverse-phase C18 HPLC (solvent program: 0−2 min: 5% B, 2−7 min: 5−15% B, 7−12 min: 15−35% B, 12−22 min: 35−60% B, 22−27 min: 60−95% B, 27−32 min: 95% B, 32−35 min: 95%−5% B, 35−45 min: 5% B. Solvents A: 100 mM ammonium formate pH 4.0, B: acetonitrile). All experiments were performed in triplicate. The substrate dependence of V/[E] was fit to a linear regression using Origin 9.0 and k_{cat}/K_M values and uncertainties were obtained from the slope.

Binding of Substrates to AzoR. AzoR (1 μM) in buffer A was stirred gently at 25 °C while titrating with azo ligands. Binding of the ligands was monitored by a diagnostic quenching of FMN_{ox} fluorescence (λ_{ex} 450 nm, λ_{em} 524 nm). All experiments were performed in triplicate. Dissociation constants were calculated by plotting the remaining fluorescence relative to the initial fluorescence ($\Delta F/F_0$) with respect to total enzyme ($[E]_t$) and total ligand ($[L]$) using eq 1 (Origin 9.0) as described previously.[52−54]

$$\frac{F}{F_0} = 1 + \frac{\Delta F}{F_0}\left(\frac{K_d + [E]_T + [L] - \sqrt{(K_d + [E]_T + [L])^2 - 4[E]_T[L]}}{2[E]_T}\right) \quad (1)$$

Molecular Docking. The structure of **4-R-Azo** was obtained from Avogadro to generate conformations of minimal energy. Water and ions were removed from the protein structure but hydrogen atoms were included. Each **4-R-Azo** ligand was docked into the active center of AzoR (PDB: 2z98) using AutoDock Vina[34] applying the standard protocol of flexible docking. The lowest-energy complex model was selected for superimposition. All structural images were generated using PyMOL (version 2.5.8).

Free Energy Calculations. Quantum chemical calculations by DFT were used to calculate the free energy and energy barrier for the

https://doi.org/10.1021/acschembio.4c00779
ACS Chem. Biol. 2025, 20, 229−237

decomposition of neutral and protonated hydrazobenzenes into their cationic intermediate and aniline anion/aniline (Scheme S5). For all reactions, the free energy change ΔG was obtained as the Gibbs free energy differences between substrate and products.

$$\Delta G_{\text{neutral}} = G_{\text{aniline anion}} + G_{\text{cationic intermediate}} - G_{\text{hydrazo}}$$

$$\Delta G_{\text{protonated}} = G_{\text{aniline}} + G_{\text{cationic intermediate}} - G_{\text{protonated-hydrazo}}$$

The energy barrier $\Delta G^{\ddagger}$ represents the free energy difference of the transition state (if found) and the hydrazo starting material. Note that transition states were only found for N−N bond lysis of protonated hydrazobenzenes with certain substituents. See Table S2 for raw data.

$$\Delta G^{\ddagger}_{\text{protonated}} = G_{\text{transition state}} - G_{\text{protonated-hydrazo}}$$

■ ASSOCIATED CONTENT

Supporting Information

The Supporting Information is available free of charge at https://pubs.acs.org/doi/10.1021/acschembio.4c00779.

Additional details on materials and experimental procedures for synthesis of substrates, preparation of the plasmid pET24a-AzoR-His6; DFT calculations; LC-MS for product identification; binding studies; kinetic measurements; molecular docking structures; and ^{1}H and ^{13}C NMR spectra for all compounds (PDF)

■ AUTHOR INFORMATION

Corresponding Author

Steven E. Rokita − *Department of Chemistry, Johns Hopkins University, Baltimore, Maryland 21218, United States;* orcid.org/0000-0002-2292-2917; Email: Rokita@jhu.edu

Authors

Yu-Ju Peng − *Department of Chemistry, Johns Hopkins University, Baltimore, Maryland 21218, United States*

Bing Xu − *Department of Chemistry, Johns Hopkins University, Baltimore, Maryland 21218, United States*

Complete contact information is available at: https://pubs.acs.org/10.1021/acschembio.4c00779

Notes

The authors declare no competing financial interest.

■ ACKNOWLEDGMENTS

Research was supported in part by a grant from the NSF (CHE-2204096). Computational studies were performed at the Advanced Research Computing at Hopkins (ARCH) core facility that is supported by the National Science Foundation (NSF: OAC-1920103).

■ DEDICATION

This article is dedicated to Professor Iwao Ojima in honor of a milestone birthday.

■ REFERENCES

(1) Jerca, F. A.; Jerca, V. V.; Hoogenboom, R. Advances and Opportunities in the Exciting World of Azobenzenes. *Nat. Rev. Chem.* **2022**, *6* (1), 51−69.

(2) Lautenschläger, C.; Schmidt, C.; Fischer, D.; Stallmach, A. Drug Delivery Strategies in the Therapy of Inflammatory Bowel Disease. *Adv. Drug Delivery Rev.* **2014**, *71*, 58−76.

(3) Sharma, R.; Rawal, R. K.; Gaba, T.; Singla, N.; Malhotra, M.; Matharoo, S.; Bhardwaj, T. R. Design, Synthesis and Ex Vivo Evaluation of Colon-Specific Azo Based Prodrugs of Anticancer Agents. *Bioorg. Med. Chem. Lett.* **2013**, *23* (19), 5332−5338.

(4) Ryan, A. Azoreductases in Drug Metabolism. *Br. J. Pharmacol.* **2017**, *174* (14), 2161−2173.

(5) Chung, K.-T. Azo Dyes and Human Health: A Review. *J. Environ. Sci. Health, Part C* **2016**, *34* (4), 233−261.

(6) Misal, S. A.; Gawai, K. R. Azoreductase: A Key Player of Xenobiotic Metabolism. *Bioresour. Bioprocess.* **2018**, *5*, No. 17.

(7) Ngo, A. C. R.; Schultes, F. P. J.; Maier, A.; Hadewig, S. N. H.; Tischler, D. Improving Biocatalytic Properties of an Azoreductase Via the N-Terminal Fusion of Formate Dehydrogenase. *ChemBioChem* **2022**, *23* (6), No. e202100643.

(8) Panwar, P.; Mahajan, P.; Kaushal, J. Microbial Bioremediation of Azo Dyes: An Environmentally Sustainable Technology. *Rem. J.* **2023**, *33* (2), 151−165.

(9) Goswami, D.; Mukherjee, J.; Mondal, C.; Bhunia, B. Bioremediation of Azo Dye: A Review on Strategies, Toxicity Assessment, Mechanisms, Bottlenecks and Prospects. *Sci. Total Environ.* **2024**, *954*, No. 176426.

(10) Verhelst, S. H. L.; Fonović, M.; Bogyo, M. A Mild Chemically Cleavable Linker System for Functional Proteomic Applications. *Angew. Chem., Int. Ed.* **2007**, *46* (8), 1284−1286.

(11) Guisán-Ceinos, S.; Rivero, A. R.; Romeo-Gella, F.; Simón-Fuente, S.; Gómez-Pastor, S.; Calvo, N.; Orrego, A. H.; Guisán, J. M.; Corral, I.; Sanz-Rodriguez, F.; Ribagorda, M. Turn-on Fluorescent Biosensors for Imaging Hypoxia-Like Conditions in Living Cells. *J. Am. Chem. Soc.* **2022**, *144* (18), 8185−8193.

(12) Zhao, X.-b.; Ha, W.; Gao, K.; Shi, Y.-p. Precisely Traceable Drug Delivery of Azoreductase-Responsive Prodrug for Colon Targeting Via Multimodal Imaging. *Anal. Chem.* **2020**, *92* (13), 9039−9047.

(13) Suzuki, H. Remarkable Diversification of Bacterial Azoreductases: Primary Sequences, Structures, Substrates, Physiological Roles, and Biotechnological Applications. *Appl. Microbiol. Biotechnol.* **2019**, *103*, 3965−3978.

(14) Bin, Y.; Jiti, Z.; Jing, W.; Cuihong, D.; Hongman, H.; Zhiyong, S.; Yongming, B. Expression and Characteristics of the Gene Encoding Azoreductase from Rhodobacter Sphaeroides As1.1737. *FEMS Microbiol. Lett.* **2004**, *236* (1), 129−136.

(15) Wang, C.-J.; Hagemeier, C.; Rahman, N.; Lowe, E.; Noble, M.; Coughtrie, M.; Sim, E.; Westwood, I. Molecular Cloning, Characterisation and Ligand-Bound Structure of an Azoreductase from *Pseudomonas Aeruginosa*. *J. Mol. Biol.* **2007**, *373* (5), 1213−1228.

(16) Ryan, A.; Laurieri, N.; Westwood, I.; Wang, C. J.; Lowe, E.; Sim, E. A Novel Mechanism for Azoreduction. *J. Mol. Biol.* **2010**, *400* (1), 24−37.

(17) Race, P. R.; Lovering, A. L.; Green, R. M.; Ossor, A.; White, S. A.; Searle, P. F.; Wrighton, C. J.; Hyde, E. I. Structural and Mechanistic Studies of *Escherichia Coli* Nitroreductase with the Antibiotic Nitrofurazone. Reversed Binding Orientations in Different Redox States of the Enzyme. *J. Biol. Chem.* **2005**, *280* (14), 13256−13264.

(18) Pitsawong, W.; Haynes, C. A.; Koder, R. L.; Rodgers, D. W.; Miller, A.-F. Mechanism-Informed Refinement Reveals Altered Substrate-Binding Mode for Catalytically Competent Nitroreductase. *Structure* **2017**, *25* (7), 978−987.

(19) Zbaida, S.; Stoddart, A. M.; Levine, W. G. Studies on the Mechanism of Reduction of Azo Dye Carcinogens by Rat Liver Microsomal Cytochrome P-450. *Chem.-Biol. Interact.* **1989**, *69* (1), 61−71.

(20) Wu, T.-H.; Su, Z.-S.; Sung, R.; Sung, K. Aza-Ortho-Quinone Methide and Its Conjugated Acid: Reactivity, Stability and Acidity. *ChemPhysChem* **2020**, *21* (4), 307−312.

(21) Rokita, S. E. Quinone Methides. In *Wiley Series on Reactive Intermediates in Chemistry and Biology*; Rokita, S. E., Ed.; Wiley Hoboken, 2009; Vol. *1*, p 431.

(22) Minard, A.; Liano, D.; Wang, X.; Di Antonio, M. The Unexplored Potential of Quinone Methides in Chemical Biology. *Bioorg. Med. Chem.* **2019**, *27*, 2298−2305.
(23) Walden, D. M.; Jaworski, A. A.; Johnston, R. C.; Hovey, M. T.; Baker, H. V.; Meyer, M. P.; Scheidt, K. A.; Cheong, P. H.-Y. Formation of Aza-Ortho-Quinone Methides under Room Temperature Conditions: Cs_2co_3 Effect. *J. Org. Chem.* **2017**, *82* (14), 7183−7189.
(24) Ito, K.; Nakanishi, M.; Lee, W.-C.; Zhi, Y.; Sasaki, H.; Zenno, S.; Saigo, K.; Kitade, Y.; Tanokura, M. Expansion of Substrate Specificity and Catalytic Mechanism of Azoreductase by X-Ray Crystallography and Site-Directed Mutagenesis. *J. Biol. Chem.* **2008**, *283* (20), 13889−13896.
(25) Nakanishi, M.; Yatome, C.; Ishida, N.; Kitade, Y. Putative Acp Phosphodiesterase Gene (Acpd) Encodes an Azoreductase. *J. Biol. Chem.* **2001**, *276* (49), 46394−46399.
(26) Qi, J.; Schlömann, M.; Tischler, D. Biochemical Characterization of an Azoreductase from Rhodococcusopacus 1CP Possessing Methyl Red Degradation Ability. *J. Mol. Catal. B:Enzym.* **2016**, *130*, 9−17.
(27) Carl, P. L.; Chakravarty, P. K.; Katzenellenbogen, J. A. A Novel Connector Linkage Applicable in Prodrug Design. *J. Med. Chem.* **1981**, *24* (5), 479−480.
(28) Erez, R.; Shabat, D. The Azaquinone-Methide Elimination: Comparison Study of 1,6- and 1,4-Eliminations under Physiological Conditions. *Org. Biomol. Chem.* **2008**, *6* (15), 2669−2672.
(29) Priewisch, B.; Rück-Braun, K. Efficient Preparation of Nitrosoarenes for the Synthesis of Azo-Benzenes. *J. Org. Chem.* **2005**, *70* (6), 2350−2352.
(30) Juodaityte, J.; Sewald, N. Synthesis of Photoswitchable Amino Acids Based on Azobenzene Chromophores: Building Blocks with Potential for Photoresponsive Biomaterials. *J. Biotechnol.* **2004**, *112* (1−2), 127−138.
(31) Ito, K.; Nakanishi, M.; Lee, W.-C.; Sasaki, H.; Zenno, S.; Saigo, K.; Kitade, Y.; Tanokura, M. Three-Dimensional Structure of Azor from *Escherichia Coli*. *J. Biol. Chem.* **2006**, *281* (29), 20567−20576.
(32) Blackadder, D. A.; Hinshelwood, C. The Kinetics of the Rearrangement and Oxidation of Hydrazobenzene in Solution. Part I. The Rearrangement and Spontaneous Oxidation. *J. Chem. Soc.* **1957**, 2898−2903.
(33) Grosjean, S.; Hodapp, P.; Hassan, Z.; Wöll, C.; Nieger, M.; Bräse, S. Synthesis of Functionalized Azobiphenyl- and Azoterphenyl-Ditopic Linkers: Modular Building Blocks for Photoresponsive Smart Materials. *ChemistryOpen* **2019**, *8* (6), 743−759.
(34) Trott, O.; Olson, A. J. Autodock Vina: Improving the Speed and Accuracy of Docking with a New Scoring Function, Efficient Optimization and Multithreading. *J. Comput. Chem.* **2010**, *31* (2), 455−461.
(35) Hansch, C.; Leo, A.; Taft, R. W. A Survey of Hammett Substituent Constants and Resonance and Field Parameters. *Chem. Rev.* **1991**, *91* (2), 165−195.
(36) Pelzer, K. M.; Cheng, L.; Curtiss, L. A. Effects of Functional Groups in Redox-Active or-Ganic Molecules: A High-Throughput Screening Approach. *J. Phys. Chem. C* **2017**, *121*, 237−245.
(37) Ryan, A.; Kaplan, E.; Laurieri, N.; Lowe, E.; Sim, E. Activation of Nitrofurazone by Azoreductases: Multiple Activities in One Enzyme. *Sci. Rep.* **2011**, *1*, No. srep00063.
(38) Romero, E.; Savino, S.; Fraaije, M. W.; Lončar, N. Mechanistic and Crystallographic Studies of Azoreductase Azoa from *Bacillus Wakoensis* A01. *ACS Chem. Biol.* **2020**, *15* (2), 504−512.
(39) Valiauga, B.; Williams, E. M.; Ackerley, D. F.; Čėnas, N. Reduction of Quinones and Nitroaromatic Compounds by *Escherichia Coli* Nitroreductase a (NfsA): Characterization of Kinetics and Substrate Specificity. *Arch. Biochem. Biophys.* **2017**, *614*, 14−22.
(40) Luján, A. P.; Bhat, M. F.; Saravanan, T.; Poelarends, G. J. Exploring the Substrate Scope and Catalytic Promiscuity of Nitroreductase-Like Enzymes. *Adv. Synth. Catal.* **2024**, *366* (22), 4679−4687.
(41) Uémura, T.; Abé, M. Études Spectrochimiques Des Matières Colorantes Dérivées De La Quinone-Imine. *Bull. Chem. Soc. Jpn.* **1937**, *12* (2), 59−70.
(42) Miner, D. J.; Kissinger, P. T. Evidence for the Involvement of N-Acetyl-P-Quinoneimine in Acetaminophen Metabolism. *Biochem. Pharmacol.* **1979**, *28* (22), 3285−3290.
(43) Dahlin, D. C.; Nelson, S. D. Synthesis, Decomposition Kinetics, and Preliminary Toxicological Studies of Pure N-Acetyl-P-Benzoquinone Imine, a Proposed Toxic Metabolite of Acetaminophen. *J. Med. Chem.* **1982**, *25* (8), 885−886.
(44) Huynh, M. T.; Anson, C. W.; Cavell, A. C.; Stahl, S. S.; Hammes-Schiffer, S. Quinone 1 E^- and 2 $E^-/2$ H^+ Reduction Potentials: Identification and Analysis of Deviations from Systematic Scaling Relationships. *J. Am. Chem. Soc.* **2016**, *138* (49), 15903−15910.
(45) Corbett, J. F. P-Phenylenediamine−Ferricyanide and P-Aminophenol−Ferricyanide Redox Systems. *J. Chem. Soc. B* **1969**, 207−212.
(46) Klotz, I. M.; Fiess, H. A.; Ho, J. Y. C.; Mellody, M. The Position of the Proton in Substituted Azobenzene Molecules. *J. Am. Chem. Soc.* **1954**, *76* (20), 5136−5140.
(47) Jaffé, H. H.; Gardner, R. W. Tautomeric Equilibria. Iv. The Basicities of Monosubstituted Azobenzenes. An Acidity Scale in 20% Ethanolic Aqueous Sulfuric Acid. *J. Am. Chem. Soc.* **1958**, *80* (2), 319−322.
(48) Eyring, H. The Activated Complex in Chemical Reactions. *J. Chem. Phys.* **1935**, *3* (2), 107−115.
(49) Evans, M. G.; Polanyi, M. Some Applications of the Transition State Method to the Calculation of Reaction Velocities, Especially in Solution. *Trans. Faraday Soc.* **1935**, *31*, 875−894.
(50) Espenson, J. H. *Chemical Kinetics and Reaction Mechanisms*; McGraw-Hill, 1981.
(51) Sun, Z.; Xu, B.; Spisak, S.; Kavran, J. M.; Rokita, S. E. The Minimal Structure for Iodotyrosine Deiodinase Function Is Defined by an Outlier Protein from Thermophilic Bacteria *Thermotoga Neapolitana*. *J. Biol. Chem.* **2021**, *297* (6), No. 101385.
(52) Warner, J. R.; Copley, S. D. Pre-Steady-State Kinetic Studies of the Reductive Dehalogenation Catalyzed by Tetrachlorohydroquinone Dehalogenase. *Biochemistry* **2007**, *46* (45), 13211−13222.
(53) McTamney, P. M.; Rokita, S. E. A Mammalian Reductive Deiodinase Has Broad Power to Dehalogenate Chlorinated and Brominated Substrates. *J. Am. Chem. Soc.* **2009**, *131* (40), 14212−14213.
(54) Kozyryev, A.; Lemen, D.; Dunn, J.; Rokita, S. E. Substrate Electronics Dominate the Rate of Reductive Dehalogenation Promoted by the Flavin-Dependent Iodotyrosine Deiodinase. *Biochemistry* **2023**, *62* (7), 1298−1306.

https://doi.org/10.1021/acschembio.4c00779
ACS Chem. Biol. 2025, 20, 229−237